Macromolecules **2004,** *37,* 5807−5813

Kinetics of Sequential Tethering in Formation of Mixed Layers

H. Huang and L. S. Penn*

Department of Chemical and Materials Engineering, University of Kentucky, Lexington, Kentucky 40506-0046

R. P. Quirk and T. H. Cheong

Department of Polymer Science, University of Akron, Akron, Ohio 44325-3909

Received December 30, 2003

ABSTRACT: This paper reports the construction of mixed tethered layers on silica substrates, in which the relative amounts of the two polymers can be controlled to the desired value. This is done by exploiting the three-regime kinetics found for tethered layer formation of single-polymer systems. Two end-functionalized polymers, different either in molecular weight or in chemical structure, were tethered sequentially: the first polymer was tethered to the surface from solution to form a mushroom layer; then, after the slow second regime had started, the solution of the first polymer was replaced with a solution of the second polymer. The original expectation was that, because the surface already contained a mushroom layer, the second polymer would exhibit only the second and third regimes of tethering. However, the second polymer exhibited its own (rapid) first regime in addition to the expected second and third regimes. It was determined that the unexpected first regime exhibited by the second polymer originated in the size difference between the two polymers in the sequence.

I. Introduction

Mixed tethered layers, i.e., containing different molecular weights or different types of polymers, have the potential to make surfaces both responsive and multifunctional in areas such as lubrication, biotechnology, and surface patterning.[1−10] Over the past decade, the interest in mixed tethered layers has been growing, both from theoretical[6,11−16] and from experimental[1−5,7−10,17−22] points of view. In the future, increasing emphasis undoubtedly will be focused on fundamental properties of mixed tethered layers as a function of composition and on optimization of the composition of mixed layers for practical applications.

Work in our laboratory is focused on construction of tethered layers of precisely known surface attachment density and composition. Tethered layers are formed by exposing the substrate to the polymer in solution. The tethering is accomplished by means of chemical bond formation between end-functionalized polymer chains and reactive sites on the surface of the substrate. Once chemically bonded to the surface, the tethered ends cannot readjust their positions, and the tethered chains cannot be displaced. The tethering process is monitored from beginning to end by means of a real-time analysis method, made quantitative by the use of internal standards. Previous work on simple systems, i.e., tethered layers composed of a single type of monodisperse polymer, revealed three distinct regimes of kinetics.[23,24] The distinct features of this type of kinetics profile suggested an approach for gaining control over the composition in mixed layers. Before describing the use of this approach for construction of mixed layers of precisely known compositions, we present a brief description of the three-regime kinetics observed for simple systems (Figure 1), which serves as the reference kinetics for the work reported in the present paper.

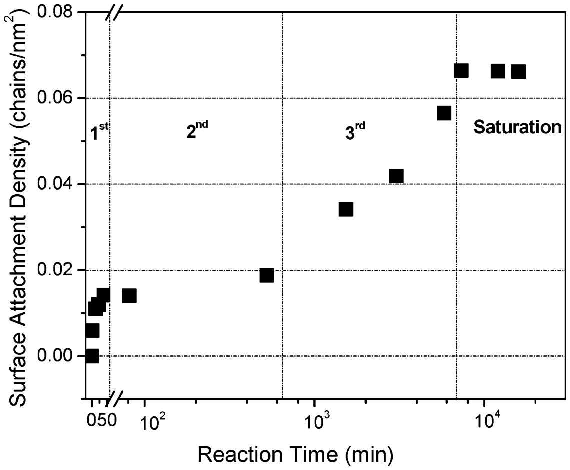

Figure 1. Surface attachment density vs time for tethering of PS-NH_2-4K. Scatter among replicate measurements is less than the size of the symbol. The horizontal axis changes from linear to log(time) at 50 min. Thin vertical lines separate the three regimes, which are identified in the figure.

Figure 1 shows a typical kinetics profile for a simple, one-component system tethered from good solvent.[25] The first regime of kinetics is fast and corresponds to construction of a mushroom layer at a rate dependent on the diffusion of the polymer chains through solution to the bare surface. As soon as the mushroom layer is complete, the first regime ends abruptly and the second regime begins. In the second regime, tethering is extremely slow because now the incoming chains have to diffuse through the mushroom layer to reach the surface. Tethering in the second regime is proportional to the logarithm of time. After a considerable length of time, the second regime is interrupted by a relative acceleration, during which the tethering is also proportional to log(time) but with a much greater slope. This increased slope establishes the accelerated tethering as a third regime of kinetics, distinct from the second. (Explanations for the origin of the third regime, which

---

* Corresponding author: phone 859-257-7897, Fax 859-323-1929, e-mail penn@engr.uky.edu.

10.1021/ma030591o CCC: $27.50

Table 1. Polymers Tethered

abbreviation	M_w	M_w/M_n	source
PS-NH_2-4K	4 000	<1.04	Quirk
PS-NH_2-15K	15 000	1.02	Quirk
PS-NH_2-44K	44 000	<1.04	Quirk
PEO-NH_2-10K	10 800	1.08	Polymer Source, Inc. (Dorval, Quebec)

Table 2. Polymers Used as Internal Standards

abbreviation	M_w	M_w/M_n	source
PS-13K	13200	1.06	Aldrich (Milwaukee, WI)
PS-2K	1940	1.04	Polymer Laboratories, Inc. (Amherst, MA)
PEO-2K	2000	1.05	Polymer Source, Inc. (Dorval, Quebec)

is not fully understood at present, are presented elsewhere.[24–26]) The third regime accounts for a large percent of the increase in tethered chain density prior to saturation, while the second regime, although lengthy, accounts for an extremely small percent of the increase. When the third regime ends at saturation, i.e., the natural cessation of tethering, the simple tethered layer is in the form of a polymer brush.

To form mixed tethered layers of controlled composition, we exploited the three-regime kinetics by using a sequential approach and switching from the first polymer in the sequence to the second polymer during the slow second regime. That is, we began the tethering process with the first polymer alone, allowing it to undergo its first regime to form a mushroom layer. As soon as the mushroom layer was complete, and the first polymer had entered its second regime (slow tethering), we removed the solution of the first polymer from the substrate and replaced it with a solution of the second polymer. We then allowed the tethering of the second polymer to proceed alone. All tethering reactions were monitored quantitatively, in real time, from beginning to end. Our hypothesis for this scheme was that the first polymer would exhibit the first regime and enter the second regime, and after it was replaced, the second polymer would exhibit the remainder of the second regime (a mushroom layer of the first polymer being present on the surface already) and then would continue through the third regime to saturation.

The present paper describes the use of sequential tethering to form mixed tethered layers of two types: bidisperse (two different molecular weights) and bicomponent (two different chemical structures). In these sequential tethering experiments, we found that the kinetics did not proceed according to our hypothesis. In addition to the expected second and third regimes, the second polymer in the sequence exhibited an unexpected first regime of its own, despite the mushroom layer of the first polymer already on the surface.

II. Experimental Section

Materials. Table 1 lists the amine-end-functionalized polymers, polystyrene (PS) and poly(ethylene oxide) (PEO), and their characteristics. Table 2 lists the inert-ended polymers (PS and PEO) used as internal standards and their characteristics. Table 3 provides the characteristics of the two silica substrates used in this work.

Synthesis of End-Functionalized Polystyrene. The synthesis of the monodisperse ω-(3-aminopropyl)polystyrene listed in Table 1 is described in detail in ref 24 and is summarized here. The *sec*-butyllithium-initiated, living anionic polymerization of styrene monomer was carried out under standard high-vacuum conditions in sealed, all-glass reactors equipped with break-seals.[27] When the polymerization was completed, i.e., when the desired molecular weight had been reached, the resulting poly(styryl)lithium was terminated with *N*-3-chloropropyl-2,2,5,5-tetramethyl-2,5,-disila-1-azapentane. Upon deprotection and reduction with $NaBH_4$, the terminal group was converted to primary amine. The resultant monodisperse, end-functionalized polymer was purified by column chromatography through silica gel and eluted sequentially with toluene and tetrahydrofuran. The fraction of chains containing primary-amine, end-functional groups was determined by titration to be >95%.

Table 3. Substrates

name	shape	surface area (m^2/g)	source
silica glass beads	spherical, nonporous	0.240[a]	Potters Industries, Inc. (Carlstadt, NJ)
silica powder	irregular, nonporous	4.84[b]	Aldrich (Milwaukee, WI)

[a] Determined by detailed analysis of SEM images (ref 24). [b] Determined by BET method with N_2 gas.

Introduction of Active Sites to the Substrate by Derivatization. The two silica substrates (beads and powder in Table 3) used in this work were derivatized to introduce epoxide reactive groups to their surfaces. The detailed procedure is presented in ref 24 and is summarized here. Both substrates were cleaned with piranha solution to remove impurities and bring out the −OH groups, rendering their surfaces identical. After being rinsed and dried, each substrate was exposed to 3-glycidoxypropyltrimethoxysilane (98%, Aldrich, Milwaukee, WI) in toluene under anhydrous conditions for 16 h. This derivatization resulted in 2.71 ± 0.24 epoxide groups/nm^2, a density of active sites considerably in excess of that needed for attachment of tethered chains.[28]

Verification of Absence of Segmental Adsorption. The tests used to verify the absence of segmental adsorption consisted of long-term exposure of the epoxide-derivatized substrate to solutions of inert-ended polymer, as described in detail in refs 24 and 25. The use of inert-ended counterparts of the end-functionalized polymers precluded the occurrence of tethering during the evaluation of segmental adsorption. The inert-ended polymer solutions in contact with the substrate were quantitatively analyzed at regular intervals to check for loss of polymer. Under the good-solvent conditions used for these tests, none of the polymers exhibited segmental adsorption to the epoxide-derivatized substrates.

Sequential Tethering Reactions. All tethering reactions were run at room temperature, under argon atmosphere, in glassware that had been previously treated with *n*-butyltrichlorosilane to lower its surface energy and prevent segmental adsorption of any polymer. The total amount of polymer in solution initially was always well in excess of the amount of polymer that could be tethered to the substrate at saturation. We describe here, as a typical example, details for only one of the many sequential reactions conducted: PS-NH_2-4K followed by PS-NH_2-44K tethered to silica beads. The reaction flask was charged with 20 mL of a solution of PS-NH_2-4K in toluene at a concentration of 0.255 mg/mL. To this solution, a known mass of monodisperse, inert-ended polystyrene of different molecular weight from the chain-end functionalized polymer was added to serve as an internal standard for quantitative analysis. The first step in the sequential tethering consisted of exposure of 18.1 g of epoxide-derivatized silica beads, with stirring, to the polymer solution. The tethering process began instantly. When the mushroom layer was completely constructed (as per real-time monitoring) and the tethering process had entered the second regime, the silica beads were separated from the solution by filtration, rinsed thoroughly by means of Soxhlet extraction to remove any nontethered polymer, and dried in a vacuum oven. The dried beads were reweighed to account for any small loss on the filter, after which they were subjected to the second step of the sequence. The second step consisted of exposure of the beads, with stirring, to a toluene solution (0.255 mg/mL) of the second polymer to be tethered. Tethering from the second

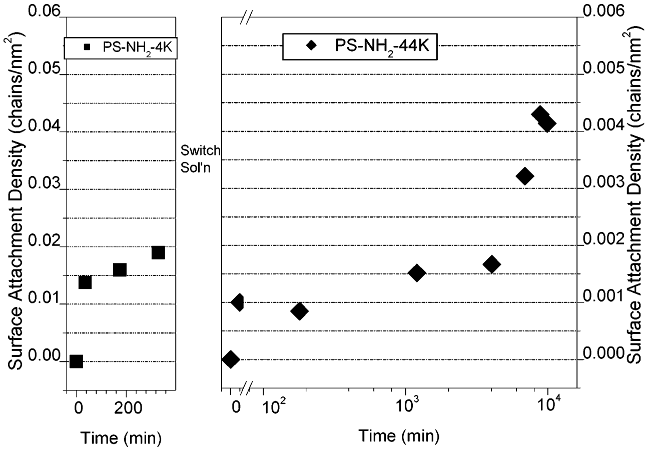

Figure 2. Surface attachment density vs time for sequential tethering of PS-NH$_2$-4K followed by PS-NH$_2$-44K. The left and right vertical axes indicate the individual surface attachment densities of PS-NH$_2$-4K and PS-NH$_2$-44K, respectively.

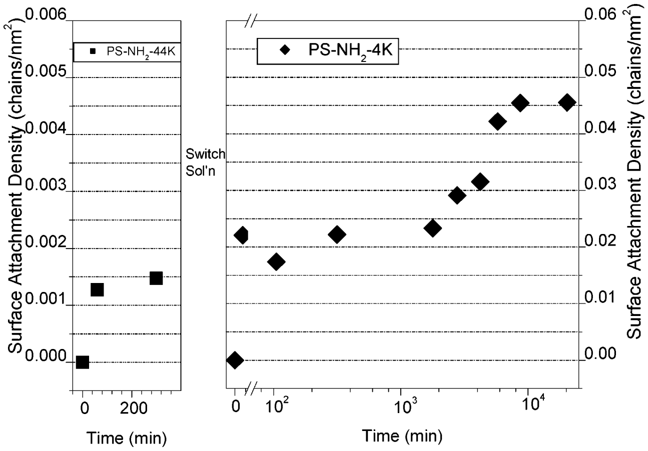

Figure 3. Surface attachment density vs time for sequential tethering of PS-NH$_2$-44K followed by PS-NH$_2$-4K. The left and right vertical axes indicate the individual surface attachment densities of PS-NH$_2$-44K and PS-NH$_2$-4K, respectively.

solution was allowed to proceed, with monitoring, until saturation was reached.

Other sequential tethering reactions were done as described above with one exception. Because the detectors used in our analysis method were not as sensitive to PEO as they were to PS, silica powder was used as the substrate when the bicomponent tethered layer involving PEO-NH$_2$-10K was constructed. In this case, the ratio of solution to substrate was increased to account for the increased surface area of the silica powder over the silica beads.

In addition, sequential tethering reactions in which the first polymer in the sequence was identical to the second polymer in the sequence were conducted. These reactions were also monitored quantitatively from beginning to end.

Quantitative Monitoring of the Tethering Reaction. The detailed procedure for the real-time monitoring of the tethering process is described in refs 24 and 25 but is summarized here. At frequent intervals during the process of tethering, small aliquots were removed from the stirring reaction mixture for analysis. Each aliquot contained both solution and substrate in order for it to represent the whole reaction mixture at the time taken. The aliquot was treated immediately with an excess of trichloroacetyl isocyanate to cap the functional ends of the polymer chains and stop further tethering. Then the beads were separated from the solution by means of a syringe filter, and the solution was quantitatively analyzed. Quantitative analysis was performed on a size exclusion chromatograph equipped with two Styragel columns (HR1 and HR3), an ultraviolet detector, and a refractive index detector. Mass of functional-ended polystyrene remaining in solution was determined with respect to that of the internal standard by comparison of peak areas on the chromatogram. (Careful choice of internal standard ensured that its elution peak would not overlap that of the functional-ended polymer being tethered.) Relative peak area at sampling time, t, was normalized by relative peak area at $t = 0$ (before addition of beads) to yield mass fraction in solution and (by difference) fraction tethered. The scatter among replicate aliquots taken at the same time did not exceed 3%.[25] Fraction tethered was multiplied by initial mass in solution to yield mass tethered at time, t. The surface attachment density, in chains/nm^2, was computed from [mass tethered × Avogadro's number]/[molecular weight × surface area of substrate].

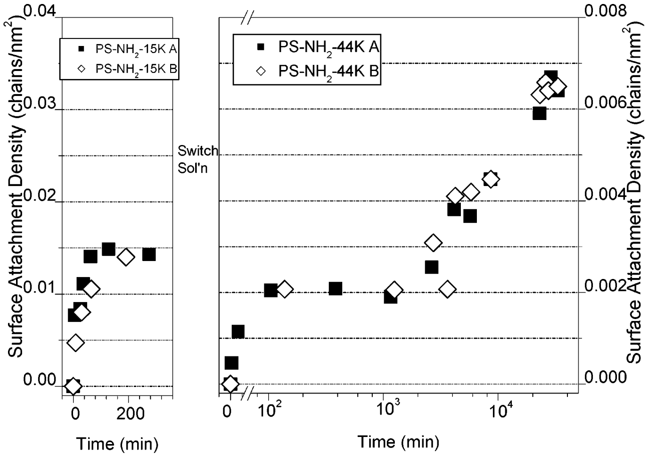

Figure 4. Surface attachment density vs time for sequential tethering of PS-NH$_2$-15K followed by PS-NH$_2$-44K. The left and right vertical axes indicate the individual surface attachment densities of PS-NH$_2$-15K and PS-NH$_2$-44K, respectively. Twin tethering reactions (open and closed symbols) were run to show run-to-run reproducibility.

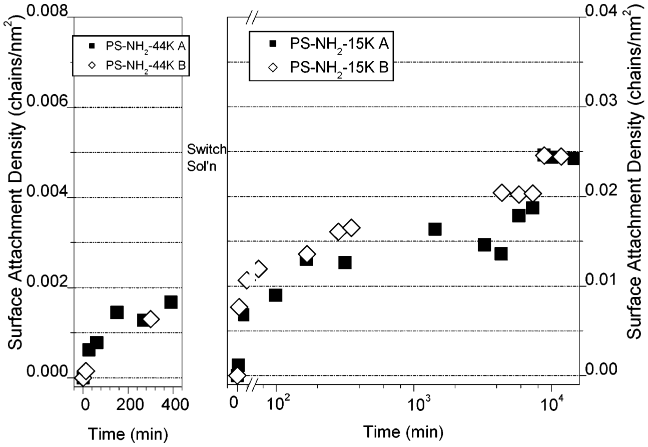

Figure 5. Surface attachment density vs time for sequential tethering of PS-NH$_2$-44K followed by PS-NH$_2$-15K. The left and right vertical axes indicate the individual surface attachment densities of PS-NH$_2$-44K and PS-NH$_2$-15K, respectively. Twin tethering reactions (open and closed symbols) were run to show run-to-run reproducibility.

III. Results and Discussion

Plots of sequential tethering reactions conducted to form bidisperse mixed layers are shown in Figures 2−5. These figures all consist of a left-hand and a right-hand part: tethering of the first polymer on the left and, after the solutions are switched, tethering of the second polymer on the right. The time axis of the left-hand part is linear, whereas the time axis of the right-hand part is linear at first and then is changed to logarithmic at

Table 4. Final Compositions of Mixed Tethered Layers

1st polymer; 2nd polymer	Σ (chains/nm^2) 1st; 2nd	no. ratio of chains short: long
PS-NH$_2$-4K: PS-NH$_2$-44K	0.019:0.0043	4.4:1
PS-NH$_2$-44K: PS-NH$_2$-4K	0.0016:0.045	28:1
PS-NH$_2$-15K: PS-NH$_2$-44K	0.015:0.0045	3.3:1
PS-NH$_2$-44K: PS-NH$_2$-15K	0.0015:0.025	17:1
PS-NH$_2$-4K: PEO-NH$_2$-10K	0.013:0.023	1:1.8

about 60 min to accommodate all the data. Note that the vertical scales at left and right in these figures are different: the scale for the polymer of lower molecular weight is an order of magnitude larger than that of the polymer of higher molecular weight. As can be seen in each of the figures, tethering of the first polymer was allowed to proceed until the mushroom layer was complete and the tethering had entered the second regime. Then the solution was switched, and tethering of the second polymer began. Tethering of the second polymer in the sequence was permitted to proceed until saturation (i.e., natural cessation of tethering) in each case. The second polymer in the sequence exhibited its own first regime, contrary to the hypothesis presented in the Introduction. This will be discussed later in this paper.

The final surface attachment densities for the two molecular weights in each of the four bidisperse layers depicted in the figures are summarized in Table 4. From the table, the observation can be made that the surface attachment density of the low-molecular-weight polymer always exceeded that of the high-molecular-weight polymer for chains of highly different sizes, no matter which was tethered first.[29] The last column shows the number ratio of short chains to long chains achieved in each final layer. Note that widely different values of short-to-long chains were achieved by simply reversing the tethering sequence, indicating the versatility of sequential tethering.

Although we allowed the tethering of the second polymer in the sequence to proceed until saturation, its tethering could have been stopped at some time before saturation was reached. Removal of the solution containing the second polymer at different time points in the process would lead to a set of different ratios of short to long chains in the final mixed tethered layer. For example, in the case of PS-NH$_2$-44K followed by PS-NH$_2$-4K, removal of the PS-NH$_2$-4K solution well before saturation would result in a ratio of short to long chains much lower than the ratio of 28:1 reported in Table 4. The only restriction on this tactic is that removal of the second polymer in the sequence cannot be done with precision during its (the second polymer's) first regime because first-regime kinetics is so fast. With this in mind, the experimenter can achieve ratios of short to long chains anywhere in the range 28:1 to 10:1 by removal of the PS-NH$_2$-4K solution at a chosen time after its first regime. The reverse sequence, PS-NH$_2$-4K followed by PS-NH$_2$-44K, provides access to ratios of short to long chains anywhere within the range 10:1 to 4.4:1 simply by removal of the second solution selected time points in the process. Overall, ratios of short to long chains spanning the range 28:1 to 4.4:1 can be achieved for a bidisperse layer of these two molecular weights.

A plot of the sequential tethering reaction conducted to form a bicomponent (PS and PEO) mixed layer is shown in Figure 6. As above, this figure consists of a left-hand and a right-hand part: tethering of the first polymer on the left and, after the solution is switched, tethering of the second polymer on the right. As can be seen in the figure, tethering of the first polymer was allowed to proceed until the mushroom layer was complete and tethering had entered the second regime. Then the solution was switched, and tethering of the second polymer began. Tethering of the second polymer in the sequence was permitted to proceed until saturation. Again, the second polymer in the sequence exhibits its own first regime, contrary to the hypothesis presented in the Introduction. This will be discussed later in this paper. The final surface attachment densities for the two components of the bicomponent layer depicted in Figure 6 are summarized in Table 4. Note that here, where the long chains (PEO) are a different chemical structure than the short chains and where the size difference is not as great as for the PS pairs in Table 4, there are more long chains than short chains.

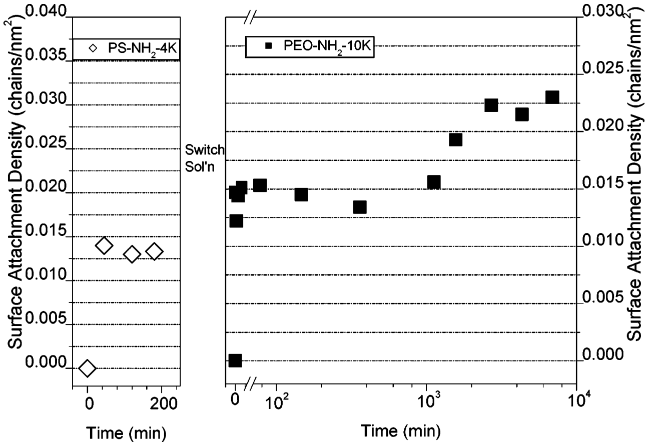

Figure 6. Surface attachment density vs time for sequential tethering of PS-NH$_2$-4K followed by PEO-NH$_2$-10K. The left and right vertical axes indicate the individual surface attachment densities of PS-NH$_2$-4K and PEO-NH$_2$-10K, respectively.

Now, we consider the unexpected display of a first regime by the second polymer in the sequence, a phenomenon that was not in accordance with the hypothesis presented in the Introduction. Consideration of the literature on random sequential deposition of regularly shaped objects to a flat surface[30−32] led us to propose that this unexpected phenomenon might be due entirely to a difference in size between the first and second polymers in the sequence. To test this proposal, we conducted some additional experiments, in which the first and second polymers tethered were identical in size. The results (Figures 7 and 8) show that the second polymer, when exposed to a substrate that already contained a mushroom layer of chains of the same size, *did not* exhibit its own first regime. Rather, the second polymer underwent extremely slow tethering, typical of second-regime behavior. Following this, the second polymer displayed the relative acceleration characteristic of the third regime and, finally, reached saturation. These additional experiments demonstrated that, when the second polymer in the sequence is the same size as the first, the second polymer exhibits only the second and third regimes of kinetics. The results of these additional experiments support our proposed explanation that the second polymer in the sequence exhibits its own first regime only if its size is different from that of the first polymer.

Again drawing on the concept of random sequential deposition, we attempt to develop an explanation, purely

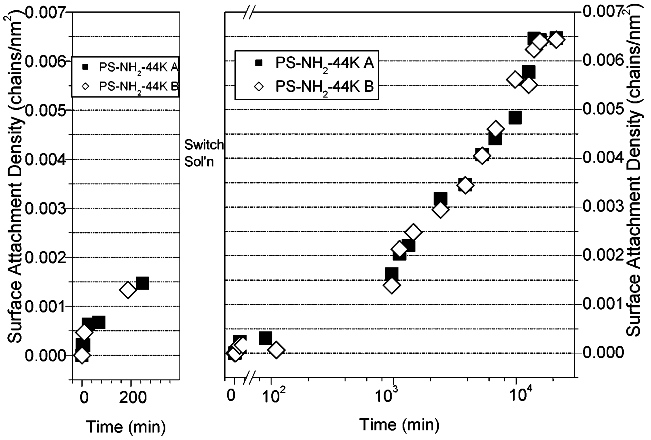

Figure 7. Surface attachment density vs time for sequential tethering of PS-NH$_2$-44K followed by PS-NH$_2$-44K. The left and right vertical axes indicate the individual surface attachment densities for the first and second parts of the sequence, respectively. Twin tethering reactions (open and closed symbols) were run to show run-to-run reproducibility.

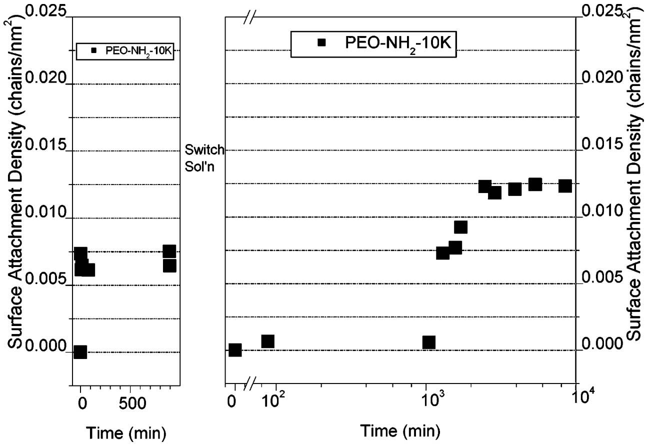

Figure 8. Surface attachment density vs time for sequential tethering of PEO-NH$_2$-10K followed by PEO-NH$_2$-10K. The left and right vertical axes indicate the individual surface attachment densities for the first and second parts of the sequence, respectively.

speculative at this time, for the first-regime kinetics exhibited by the second polymer in sequential tethering of polymers of different sizes. In the random deposition of rigid circular objects of a given uniform size, deposition occurs easily and rapidly until a jamming limit is reached.[30,31] This is the point at which no further objects can be deposited without overlap. Mathematically, the surface coverage at the jamming limit is about 55%, leaving 45% of the substrate surface area empty.[30,31] After the jamming limit has been reached, continued deposition of the same-sized objects cannot be done without a relaxation of the original constraints on the system. However, a change to rigid circular objects of a smaller size would circumvent this constraint. These smaller objects could be deposited into the empty spaces between the larger objects just as easily as the larger objects were deposited onto the bare surface before their jamming limit was reached.[31] In construction of a tethered layer from polymer chains, a completed mushroom layer can be regarded as equivalent to a surface that contains objects deposited to their jamming limit.[33] We first consider a mushroom layer comprised of tethered chains of high molecular weight, i.e., large mushrooms. Once the mushroom layer is complete, subsequent tethering of polymer chains of the same large size is difficult, but tethering of smaller polymer chains to the empty areas between large chains would be expected to occur easily, giving an apparent first regime for the second—and smaller—polymer in the sequence. Then, when the smaller polymer had filled the empty areas, it would it embark on its own second regime.

The reverse case, in which a large polymer is tethered second in the sequence and displays its own first regime, also exploits the relative difference in size. In this case, the first polymer tethered is of low molecular weight and the mushroom layer is comprised of small mushrooms. These, too, are at their jamming limit, and 45% of the surface of the substrate is unoccupied, in the form of many, very small empty areas. A large polymer chain approaching a mushroom layer of small chains is approaching a layer that is shallow relative to its own large size. Entry into an empty area of the mushroom layer by the functionalized free end of a large polymer chain would require only a small thermal excursion relative to the size of the large chain. Such a thermal excursion is relatively easy for two reasons; the free ends of a chain are able to respond more rapidly to thermal fluctuations than are the internal segments, and the free ends tend to spend more time at the periphery of the coil than buried inside it.[34] Thus, large chains could be tethered quite rapidly to the empty areas of a mushroom layer of small chains, giving an apparent first regime for the second—and larger—polymer in the sequence.

Finally, it is of interest to consider the configurations of the chains in the mixed tethered layers we constructed, i.e., in good solvent and in which the second polymer in the sequence was tethered to saturation. This requires introduction of the notion of stratification of a bidisperse tethered layer into inner and outer strata, parallel to the substrate surface. This notion was proposed first in theoretical studies[11−14] and was later verified by neutron reflection studies on bidisperse layers prepared in other laboratories.[14,18−20] The inner stratum, adjacent to the surface of the substrate, is composed of the short chains plus that portion of the long chains closest to their attachment points. The outer stratum, farther away from the surface, is composed of the remaining lengths of the long chains, which extend beyond the short chains.

The configurations of the chains in each stratum can be evaluated separately by use of two quantities: d, the average distance between attachment points of the chains (computed from experimental data), and R_g, the radius of gyration of analogous *free* chains in a good solvent.[35−37] The commonly used qualitative criterion, $d < 2R_g$, implies that the polymer chains are stretched into a brush configuration.[38] For the inner stratum, d is taken to be the average distance between attachment points of all chains—long and short—tethered to the surface, and R_g used for the comparison is the radius of gyration of the *shorter* chains in the mixed layer. Table 5 shows that the only case in which $d < 2R_g$ is for mixed layers comprised of PS-NH$_2$-15K and PS-NH$_2$-44K, tethered in either order; this indicates that the chains in the inner stratum are sufficiently crowded to be stretched away from the surface of the substrate. For all other combinations $d > 2R_g$, which indicates that the chains in the inner stratum have enough room to be in the mushroom configuration.

Table 5. Data for Evaluating Configurational Status of Mixed Layers

		inner stratum		outer stratum	
1st polymer; 2nd polymer	Σ, chains/nm^2 1st; 2nd	*d*, nm all chains	2R_g, nm short chains	*d*, nm long chains	2R_g, nm long chains
PS-NH$_2$-4K: PS-NH$_2$-44K	0.019:0.0043	6.55	4.14	15.2	14.8
PS-NH$_2$-44K: PS-NH$_2$-4K	0.0016:0.045	4.63	4.14	25.0	14.8
PS-NH$_2$-15K: PS−NH$_2$−44K	0.015:0.0045	7.16	8.56	14.9	12.4
PS-NH$_2$-44K: PS−NH$_2$−15K	0.0015:0.025	6.14	8.56	25.8	12.4
PS-NH$_2$-4K: PEO-NH$_2$-10K	0.013:0.023	5.27	4.14	6.59	5.79

For the outer stratum, d is taken to be the average distance between attachment points of the long chains only, and R_g used for the comparison is the radius of gyration computed for that portion of the chain that extends beyond the inner stratum.[12] Table 5 shows that when the long chains were tethered first in the sequence, the outer strata (composed of the long chains only) are clearly in the mushroom configuration ($d > 2R_g$). This was the expected result because when long chains were first in the sequence, their tethering was stopped after completion of the mushroom layer. By contrast, when short chains were tethered first in the sequence, $d \approx 2R_g$, which indicates a borderline case between mushroom and brush for the outer stratum. If the suggestion[11] is followed that a disproportionately large amount of the contour length resides in the outer stratum to gain entropy, while the residual length in the inner stratum is stretched, the calculated values of $2R_g$ become slightly larger, so that $d < 2R_g$. Stretching of the chains in the outer stratum would be the expected result from a sequence in which long chains were second and were tethered to saturation because stretching plays a role in bringing the tethering to a natural halt (saturation).[39] It should be noted that, in all these examples, the tethering of the second polymer in the sequence was allowed to come to a halt naturally, with ample numbers of epoxide reactive sites still remaining on the substrate, as discussed in previous publications.[25,28]

IV. Conclusions

Several mixed tethered layers, composed of polymers either of two molecular weights or two chemical structures, were constructed. Mixed layers of known and controlled compositions were achieved by exploiting the unique, three-regime kinetics established previously for monodisperse, single-component tethered layers. The two polymers for the mixed layer were tethered sequentially; the first polymer was allowed to form a mushroom layer, and then, when its tethering rate slowed down, it was replaced with the second polymer. The second polymer was then tethered to saturation. These experiments showed that a wide range of ratios of the two polymers in the mixed layer could be achieved by means of a sequential tethering approach. Our hypothesis for the sequential tethering was that once the first polymer had exhibited the first regime, the second polymer in the sequence would exhibit only a second and third regime, giving a total of three regimes, similar to the tethering of a simple, one-polymer system. However, contrary to our hypothesis, the second polymer in the sequence exhibited an unexpected *first* regime in addition to the expected second and third regimes. We determined that the unexpected first regime originated in the size difference between the first and second polymers in the sequence.

Acknowledgment. This work was supported in part by NSF Grants CTS-9911181 and CTS-0218977. The authors also gratefully acknowledge the help of Ms. Erin Fulchiero, Bryn Mawr College, supported by NSF Grant DMS-0097692 and an equipment grant from the University of Kentucky.

References and Notes

(1) Minko, S.; Muller, M.; Motornov, M.; Nitschke, M.; Grundke, K.; Stamm, M. *J. Am. Chem. Soc.* **2003**, *125*, 3896−3900.
(2) Ionov, L.; Minko, S.; Stamm, M.; Gohy, J. F.; Jerome, R.; Scholl, A. *J. Am. Chem. Soc.* **2003**, *125*, 8302−8306.
(3) Houbenov, N.; Minko, S.; Stamm, M. *Macromolecules* **2003**, *36*, 5897−5901.
(4) Motormov, M.; Minko, S.; Eichhorn, K. J.; Nitschke, M.; Simon, F.; Stamm, M. *Langmuir* **2003**, *19*, 8077−8085.
(5) Minko, S.; Usov, D.; Goreshnik, E. J.; Stamm, M. *Macromol. Rapid Commun.* **2001**, *22*, 206−211.
(6) Zhulina, E.; Balazs, A. C. *Macromolecules* **1996**, *29*, 2667−2673.
(7) Lemieux, M.; Usov, D.; Minko, S.; Stamm, M.; Shulha, H.; Tsukruk, V. V. *Macromolecules* **2003**, *36*, 7244−7255.
(8) Minko, S.; Luzinov, I.; Luchnikov, V.; Muller, M.; Patil, S.; Stamm, M. *Macromolecules* **2003**, *36*, 7268−7279.
(9) Julthongpiput, D.; Lin, Y. H.; Teng, J.; Zubarov, E. R.; Tsukruk, V. V. *Langmuir* **2003**, *19*, 7832−7836.
(10) Siderenko, A.; Minko, S.; Schenk-Meuser, K.; Duschner, H.; Stamm, M. *Langmuir* **1999**, *15*, 8349−8355.
(11) Lai, P. K.; Zhulina, E. B. *Macromolecules* **1992**, *25*, 5201−5207.
(12) Dan, N.; Tirrell, M. *Macromolecules* **1993**, *26*, 6467−6473.
(13) Chen, H.; Chakrabarti, A. *Phys. Rev. E* **1995**, *52*, 3915−3921.
(14) Currie, E. P. K.; Wagemaker, M.; Cohen-Stuart, M. A.; van Well, A. A. *Macromolecules* **1999**, *32*, 9041−9050.
(15) Minko, S.; Muller, M.; Usov, D.; Scholl, A.; Froeck, C.; Stamm, M. *Phys. Rev. Lett.* **2002**, *88*, 035502-1−035502-4.
(16) Muller, M. *Phys. Rev. E* **2002**, *65*, 030802-1−030802-4.
(17) Dhoot; S.; Tirrell, M. *Macromolecules* **1995**, *28*, 3692−3701.
(18) Kent, M. S.; Factor, B. J.; Satija, S.; Gallagher, P.; Smith, G. S. *Macromolecules* **1996**, *29*, 2843−2849.
(19) Levicky, R.; Koneripalli, N.; Tirrell, M.; Satija, S. *Macromolecules* **1998**, *31*, 2616−2621.
(20) Goedel, W. A.; Luap, C.; Oeser, R.; Lang, P.; Braun, C.; Steitz, R. *Macromolecules* **1999**, *32*, 7599−7609.
(21) Kilbey, S. M.; Watanabe, H.; Tirrell, M. *Macromolecules* **2001**, *34*, 5249−5259.
(22) Minko, S.; Patil, S.; Datsyuk, V.; Simon, F.; Eichhorn, K. J.; Motornov, M.; Usov, D.; Tokarev, I.; Stamm, M. *Langmuir* **2002**, *18*, 289−296.
(23) Penn, L. S.; Hunter, T. F.; Lee, Y.; Quirk, R. P. *Macromolecules* **2000**, *33*, 1105−1107.
(24) Penn, L. S.; Huang, H.; Sindkhedkar, Rankin, S. E.; Chittenden, K.; Quirk, R. P.; Mathers, R. T.; Lee, Y. *Macromolecules* **2002**, *35*, 7054−7066.
(25) Huang, H.; Penn, L. S.; Quirk, R. P.; Cheong, T. H. *Macromolecules* **2004**, *37*, 516−523.
(26) Huang, H.; Rankin, S. E.; Penn, L. S.; Quirk, R. P.; Cheong, T. H. *Langmuir*, in press.
(27) Morton, M.; Fetters, L. J. *Rubber Chem. Technol.* **1979**, *48*, 359−365.
(28) Lin, R.; Quirk, R. P.; Kuang, J.; Penn, L. S. *J. Adhes. Sci. Technol.* **1996**, *10*, 341−349.
(29) If one computes the value for area/monomer for the mushroom layers formed by the first polymer in each of the sequences shown in Figures 2−4, one notices that area/monomer for PS-NH$_2$-15K is lower than the values for PS-

NH_2-4K and PS-NH_2-44K, even though the surface attachment density, Σ, of the PS-NH_2-15K is intermediate to those of the other two, as expected. We note that in numerous tethering experiments the PS-NH_2-15K always yields a slightly lower area per monomer than its higher and lower MW counterparts. While, intuitively, one would expect a trendlike behavior, the detailed behavior of area/monomer with molecular weight at the relatively low molecule weights used in our studies is not known at the present time. We also note that there is precedent in the literature for a nonmonotonic value of area per monomer with increasing molecular weight (Koutsos, V.; van der Vegte, E. W.; Hadziioannou, G. *Macromolecules* **1999**, *32*, 1233−1236).

(30) Evans, J. W. *Rev. Mod. Phys.* **1993**, *65*, 1281−1329.

(31) Hinrichsen, E. L.; Feder, J.; Jossang, T. *Geometry of Random Sequential Adsorption;* Report No. 85-22; Institute of Physics, University of Oslo, 1985.

(32) Talbot, J.; Tarjus, G.; Van Tassel, P. R.; Viot, P. *Colloids Surf. Sci. A*: *Phys. Eng. Aspects* **2000**, *165*, 287−324.

(33) Douglas, J. F.; Schneider, H. M.; Frantz, P.; Lipman, R.; Granick, S. *J. Phys.: Condens. Matter* **1997**, *9*, 7699−7718.

(34) This can be visualized from a molecular dynamics simulation of the thermal motions of a polymer chain, which can be downloaded from an educational Web site provided by Boston University as the Virtual Molecular Dynamics Laboratory at http://polymer.bu.edu/vmdl/Installers/universal/install.htm.

(35) Flory, P. J. *Statistical Mechanics of Chain Molecules*; Wiley-Interscience: New York, 1969; Chapter 2.

(36) Flory, P. J. *Principles of Polymer Chemistry*, Cornell University Press: Ithaca, NY, 1953; Chapter 14.

(37) Rubenstein, M.; Colby, R. H. *Polymer Physics*; Oxford University Press: New York, 2003; Chapter 2.

(38) Fleer, G. J.; Cohen Stuart, M. A.; Scheutjens, J. M.; Cosgrove, T.; Vincent, B. *Polymers at Interfaces*; Chapman & Hall: London, 1993; Chapter 8.

(39) Milner, S. T. *Science* **1991**, *251*, 905−914.

MA030591O